High sensitivity graphene-based MEMS pressure sensor on perforated thin SiN_x membrane

Qiugu Wang, Wei Hong, Liang Dong, Jay M. Bjerke and Mark Juetten

Iowa State University, IA, USA, qgwang@iastate.edu, whong@iastate.edu, ldong@iastate.edu, jbjerke@iastate.edu, mjuetten@iastate.edu

ABSTRACT

We present a microelectromechanical systems (MEMS) graphene-based pressure sensor realized by transferring a large area, few-layered graphene on a suspended SiN_x thin membrane perforated by a periodic array of micro-through-holes. Each through-hole is covered by a circular drum-like graphene layer, namely graphene "microdrum". The uniquess of the sensor design is that introducing the through-hole arrays into the supporting nitride membrane allows generating an increased strain in the graphene membrane over the through-hole array by local deformations of the holes under an applied differential pressure. Electromechanical measurements show a gauge factor of 4.4 for the graphene membrane and a sensitivity of 2.8×10^{-5} $mbar^{-1}$ for the pressure sensor with a good linearity over a wide pressure range. The present sensor outperforms most existing MEMS-based small footprint pressure sensors using graphene, silicon, and carbon nanotubes as sensitive materials, due to the high sensitivity.

Keywords: Graphene, MEMS, pressure sensor, through-hole

1 INTRODUCTION

Graphene [1] is a promising material for applications in micro-electro-mechanical systems (MEMS) owing to its atomic thickness, fast electron mobility, and high Young's modulus. Because graphene is impermeable to standard gases including helium and has strong adhesion to silicon oxide (SiO_2) substrate, graphene has been suggested as an atomic thick pressure sensor [2]. Recently, chemical vapor deposition (CVD) has enabled large-area uniform formation of single and few-layer graphene sheets on different substrates [3]. This ability, in conjunction with well-developed patterning and transferring methods for graphene sheets [4], have opened up new opportunities of developing graphene-based sensors and actuators. Strain induced electrical-mechanical coupling in graphene are widely reported [5]. At present only a few MEMS-based graphene pressure sensors have been demonstrated [2, 6, 7].

In this paper, we report on a high sensitivity, small area MEMS pressure sensor using few-layered graphene on a flexible perforated SiN_x thin membrane (Fig. 1a and b). The SiN_x membrane acts as a supporting layer for the graphene membrane and has a periodic array of microsized through-holes (Fig. 1d). Therefore, an array of circular drum-like graphene structures are formed above these through-holes (Fig. 1e). The introduction of the microsized through-hole array into the supporting membrane allows generating an increased membrane strain locally in the graphene layer over the holes (Fig. 1c). Further reasons which add to obtain a large strain change in graphene and thus a high pressure sensitivity of the sensor include the facts that the perforated membrane deflects more than an imperforated counterpart membrane of the same dimensions, and that the graphene microdrums are pressurized to bulge up under an applied pressure.

2 DEVICE DESIGN AND TESTING

To proof this device concept, we fabricated a perforated SiN_x square membrane (490×490 μm^2) by depositing 200 ± 2.7 nm thick nitride on a silicon substrate and patterning with 2.5 µm-diameter holes, followed by removing silicon below the membrane. Subsequently, a few-layered graphene membrane was transferred on the perforated nitride membrane. The nitride membrane was pretreated with oxygen plasma to improve van der Waals interactions between the graphene and nitride membrane. After that, the graphene resistor pattern was patterned with the help of a metal shadow mask. Lastly, metal contacts were formed by using shadow mask evaporation of gold. To test the fabricated device, the backside of the device was adhered to the outlet of a plexiglass-based air channel. Air pressure was applied from the inlet of the air channel using a programmable syringe pump. A commercial differential pressure sensor was used to measure differential pressures applied across the sensitive membrane. The piezoresistive effect of the graphene sensor was measured with a Wheatstone bridge circuit and analyzed using the equivalent circuit approximation [8].

Fig. 1d shows the surface coverage of graphene on the perforated nitride membrane suspended over the micromachined silicon base. Only a few pinholes were observed in the graphene membrane (see arrows in Fig. 1e). We also performed contact profile measurement (Fig. 1f). Fig. 1g shows that the measured deflection of the composite membrane is 14.1 µm at a differential pressure of 400 mbar.

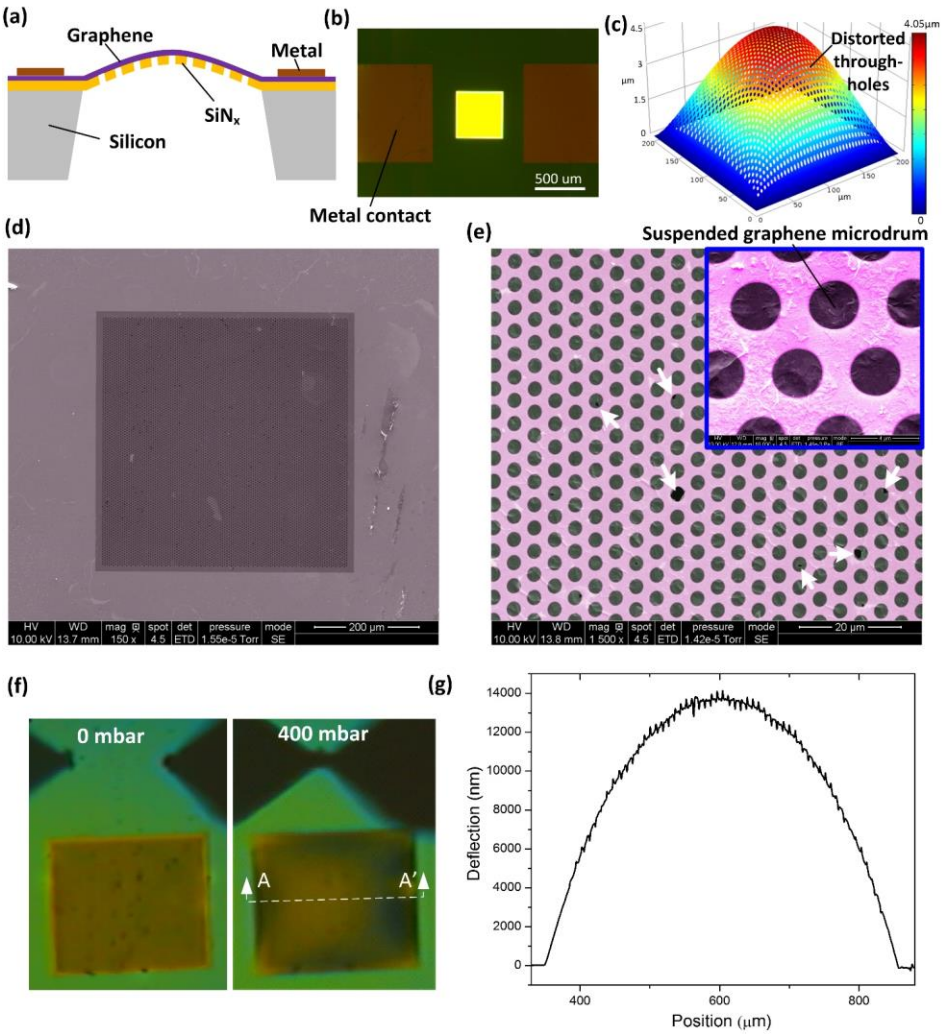

Figure 1. (a) Schematic of the proposed MEMS pressure sensor. (b) Optical image of the fabricated pressure sensor. (c) Simulated deformation of the membrane and shape distortion of the through-holes. (d, e) SEM images of the graphene membrane on the perforated SiN_x membrane. The white arrows in (e) indicate the locations of some pinholes in the graphene. (f) Optical images of the sensor before and after applying a differential pressure of 400 mbar. (g) Measured surface profile of the graphene-perforated SiNx composite membrane along the line A-A' across the center of the membrane. The measurement was conducted using Ambios XP-100 Stylus contact surface profiler.

3 RESULTS AND DISCUSSION

Fig. 2a shows the output voltage normalized to the input voltage of the device responding to an increase in step-like differential pressure. The output voltage rose with increasing air pressure applied to the graphene-perforated membrane. At a differential pressure of 350 mbar, 0.067% relative change was observed at the output voltage, corresponding to 0.97% change in the resistance.

Fig. 2b show the results of cyclic pressure testing for the device. Upon applying an air pressure, the output voltage was able to quickly follow the sudden increase of the internal pressure and then go back to the baseline.

Fig. 2c shows the response of V_{out}/V_{in} to applied differential pressure. In order to evaluate the influence of temperature on the sensitivity, the device was measured at different temperatures. At 23 °C, a good linearity was observed and the sensitivity of 3.88×10^{-5} mV/mbar was obtained. The gauge factor, GF of graphene for the sensor was estimated by $G = \frac{\Delta R/R}{\Delta L/L}$ = 4.4 at 350 mbar. As the environmental temperature increased from room temperature to 70 °C, the response of V_{out}/V_{in} showed an overall increase and had a good linear dependence on the applied pressure. The slopes of the linearly fitted curves at different temperatures were almost unchanged. At 70 °C, the resistance of graphene increased by 2.3% compared to that at 23 °C, as seen in Fig. 3d.

Next, we conducted mechanical simulations to illustrate strain distributions of membranes using COMSOL Multiphysics. Under 500 mbar differential pressure, the imperforated membrane had the maximum areal strain of

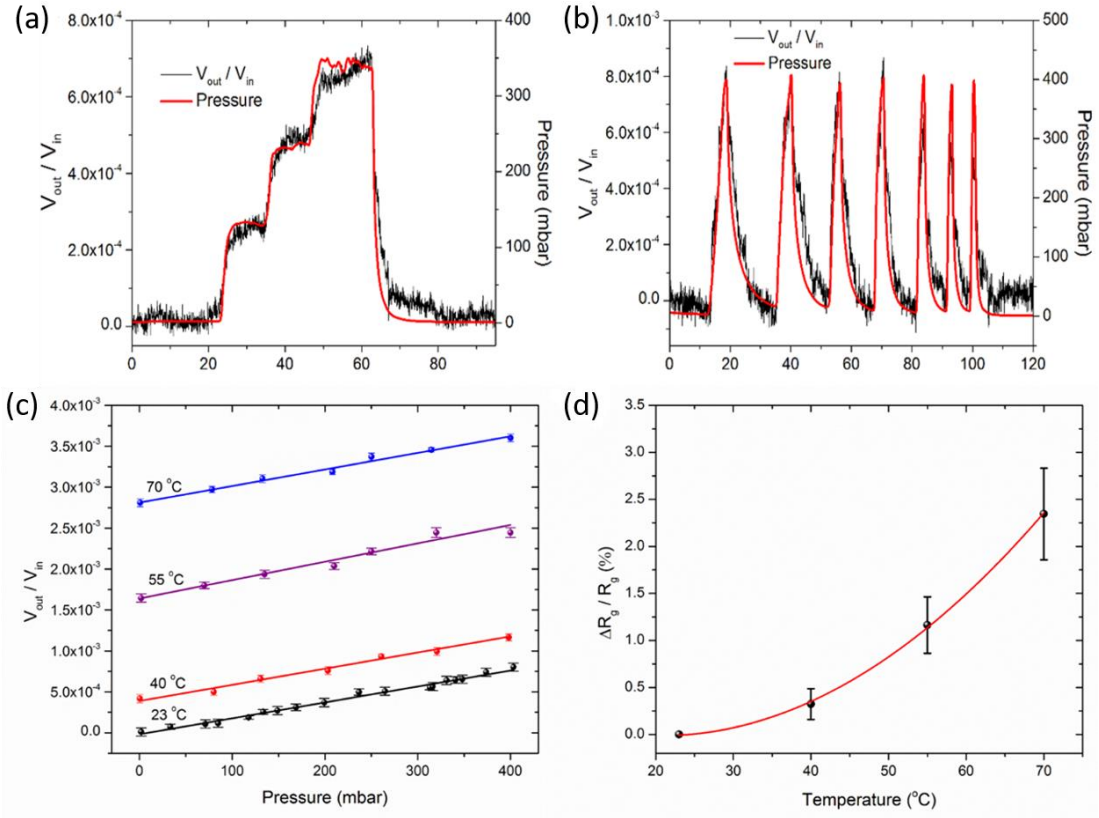

Figure 2: (a) Voltage response of the device to step like increasing differential pressures. (b) Voltage response of the device to rapid increase and gradual decrease in applied differential pressure. (c) Static voltage response of the sensor as function of applied differential pressure at the temperatures of 23ºC, 40ºC and 70ºC. (d) The change of graphene resistance versus different temperature before applying differential pressure. The resistance of graphene R_g was measured to be 1215 Ω at 23 ºC.

0.14% at the center of the membrane with the deflection of 3.49 µm (Fig. 3a). For the perforated membrane, the maximum areal strain in the graphene layer over the holes reached 0.34% at the center of the membrane with the maximum deflection of 4.13 µm. Therefore, the maximum strain in the hole areas was as high as 2.27 times that occurred in the non-hole areas of the perforated membrane. Furthermore, the average areal strain along the line across the center of the perforated and imperforated membranes was 0.203% and 0.12%, respectively (Fig. 3c). The average strain in the perforated membrane increases by 62.4% (0.203 % vs. 0.12 %) due to the introduction of the through-holes into the SiN_x membrane.

We further investigated the effect of the hole diameter and period on the mechanical properties of the membrane. As shown in Fig. 3c, given the same filling factor, the period of holes has almost no influence on the deflection and average areal strain of the membrane. As the filling factor increases, the deflection and the average areal strain of the membrane continuously grows. While the sensitivity of the device can be improved further by introducing larger size holes in the SiN_x membrane, the current design is considered safe and conservative and able to compromise the sensitivity and robustness of the device.

Table 1 compares our device with the recently reported graphene-based MEMS/NEMS pressure sensors. Generally, the sensitivity of piezoresistive pressure sensors can be calculated using $S = \frac{\Delta R}{R / P}$. Our sensor has the sensitivity of 2.8×10^{-5} $mbar^{-1}$ which outperforms most of the reported graphene, polysilicon, and carbon nanotube based MEMS/NEMS pressure sensors. Specifically, the present sensitivity is higher than 2.96×10^{-6} $mbar^{-1}$ of the standalone graphene membrane-based sensor [2] and 6.67×10^{-6} $mbar^{-1}$ of the sensor using the graphene meander patterns on imperforated SiN_x membrane [6].

4 CONCLUSIONS

We have demonstrated a graphene based small area MEMS pressure sensor formed by transferring large area CVD-grown graphene onto a suspended SiN_x membrane perforated by an array of through-holes. The large voltage response of the sensor was majorly due to the large strain change of the graphene suspended over the through-holes under applied differential pressure across the membrane. The measured sensitivity has demonstrated that the devised

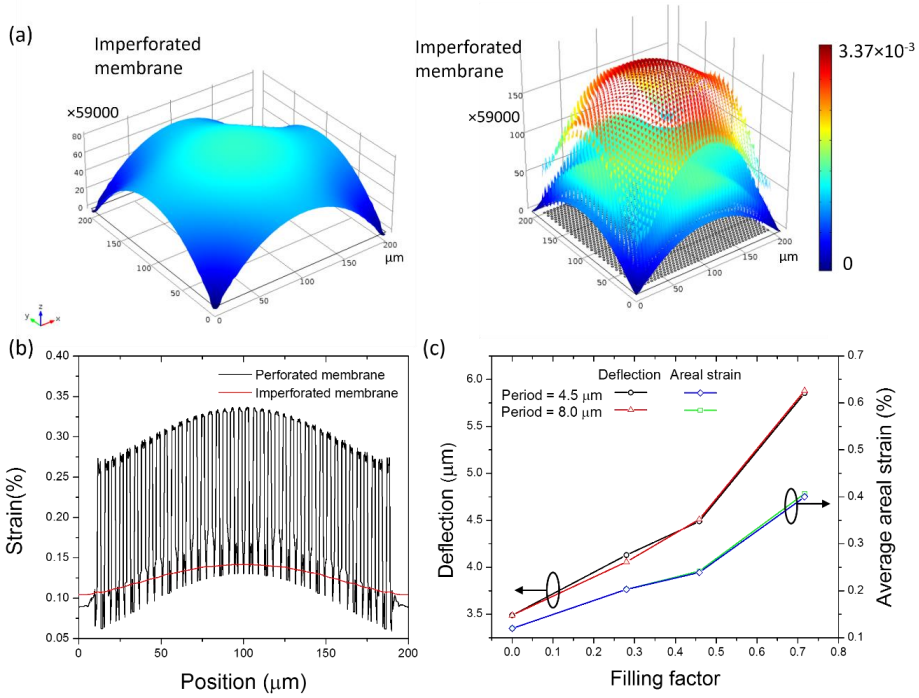

Figure 3: (a) Simulated areal strain under a differential pressure of 500 mbar for the imperforated (left) and perforated (right) membranes. The *z* coordinate and the color scale show the amplitude of the areal strain. (b) The areal strain along the line across the center of the perforated and imperforated membranes. (c) Deflection and average areal strain along the line across the center of the membrane versus different filling factor of the device. The filling factor is defined as the ratio between the area of holes and the membrane.

Table 1. Performance comparison among MEMS pressure sensors

Device structure	Dimensions	Sensitivity	Reference
Graphene on 200 nm thick perforated SiN_x	490×490	2.8×10^{-5}	This work
Suspended graphene	6×64	2.96×10^{-6}	Smith et al., Nano Lett. 2013
Graphene meander on 100 nm thick SiN_x	280×280	6.67×10^{-6}	Zhu et al., Appl. Phys. Lett.
Graphene on fixed perforated layer on silicon	110×220	0.88×10^{-6}	Hurst et al., Transducers, 2013
Carbon nanotubes	100×100	1.06×10^{-6}	Hierold et al., Sens. Actuator A,
100 μm thick polysilicon membrane	100×100	1.5×10^{-6}	Kalvesten et al., MEMS, 1998
30 μm thick silicon membrane	470×470	3.2×10^{-6}	Zhang et al., IEEE Sens. J., 2007
4 μm thick polysilicon membrane	400×400	1.29×10^{-6}	Yang, et al.,Tamkang J. Sci.

new pressure sensor structure excels in providing high sensitivity that outperforms many other existing graphene based counterpart sensors.

5 ACKNOWLEDGEMENTS

This work was supported in part by United States National Science Foundation under Grant # ECCS-0954765 and Iowa Department of Transportation. The authors thank Dr. Ashraf Bastawros for 3D optical profile measurement, and Seval Oren and Dr. Warren Straszheim for SEM imaging.

REFERENCES

[1] S. V. Morozov, et al, Phys. Rev. Lett., 100, 016602, 2008.
[2] A. D. Smith, et al, Nano Lett., 13, 3237-3242, 2013.
[3] A. Reina, et al, J. Phys. Chem. C, 112, 17741-17744, 2008.
[4] J. W. Suk, et al, Acs Nano, 2011, 5, 6916-6924, 2011.
[5] Y. Lee, et al, Nano Lett., 10, 490-493, 2010.
[6] S. E. Zhu, et al, Appl. Phys. Lett., 102, 161904, 2013.
[7]H. Hosseinzadegan, et al, IEEE MEMS 2012 Conference, 611-614, 2012.
[8] Q. Wang, et al, Nanoscale, 8, 7663-7671, 2016.